Electronic Supporting Information Submitted For :

Redox Control of Molecular Motions in Bipyridinium Appended Calixarenes

Adriana Iordache[a], Ramu Kanappan[a], Estelle Métay[b], Marie-Christine Duclos[b], Stéphane Pellet-Rostaing[b], Marc Lemaire[b], Anne Milet[c], Eric Saint-Aman[a]* and Christophe Bucher[a,d]*

[a]Département de Chimie Moléculaire (UMR5250), Laboratoire de Chimie Inorganique Rédox, Université Joseph Fourier/CNRS, Grenoble-France.
[b]Institut de Chimie et Biochimie Moléculaires et Supramoléculaires (UMR5246), Université Claude Bernard Lyon 1/CNRS, Domaine Scientifique de la Doua, Villeurbanne-France.
[c]Département de Chimie Moléculaire (UMR5250), Laboratoire de Chimie Théorique, Université Joseph Fourier/CNRS, Grenoble-France.
[d]Laboratoire de Chimie (UMR5182), École Normale Supérieure de Lyon/CNRS, Lyon-France.

Table of contents:

Fig. ESI 1 : HRMS spectrum of compound **6**$(PF_6)_4$

Calculated mass for **6**$(PF_6)_4$: $C_{72}H_{88}F_{24}N_4O_4P_4$; Exact Mass: 1652,54
Calculated mass for $[\mathbf{6}(PF_6)_3]^+$: $C_{72}H_{88}F_{18}N_4O_4P_3$; Exact Mass: 1507,57
Calculated mass for $[\mathbf{6}(PF_6)_3]^{2+}$: $C_{72}H_{88}F_{12}N_4O_4P_2$; Exact Mass: 1362,61
Calculated mass for $[\mathbf{6}(PF_6)_3]^{3+}$: $C_{72}H_{88}F_6N_4O_4P$; Exact Mass: 1217,64

CENTRE COMMUN DE SPECTROMETRIE DE MASSE

Analysis Info

Analysis Name	QTOF_130328_04_CB11X184.d		
Method	MS_inf_TL_50_1000_Pos_CCSM_2.m	Acquisition Date	3/28/2013 1:19:34 PM
Comment		Instrument / Ser#	micrOTOF-Q II 10231

Acquisition Parameter

Source Type	ESI	Ion Polarity	Positive	Set Nebulizer	0.4 Bar
Focus	Not active	Set Capillary	1300 V	Set Dry Heater	200 °C
Scan Begin	50 m/z	Set End Plate Offset	-500 V	Set Dry Gas	4.0 l/min
Scan End	1000 m/z	Set Collision Cell RF	50.0 Vpp	Set Divert Valve	Waste

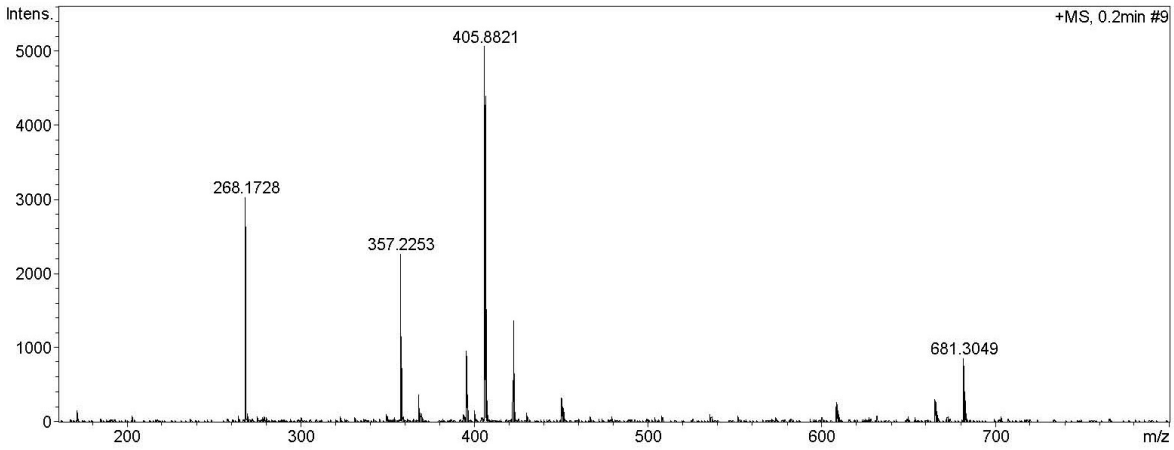

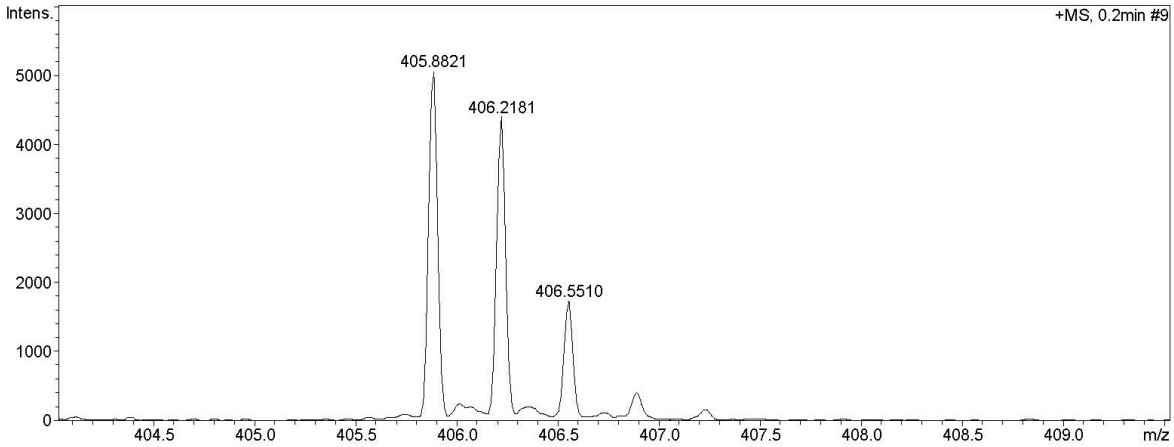

Meas. m/z	Formula	m/z	err [ppm]	mSigma
405.8821	C 72 H 88 F 6 N 4 O 4 P	405.8810	-2.7	50.6

Bruker Compass DataAnalysis 4.0 Page 1 of 1

Fig. ESI 2 : ^{1}H NMR spectrum of **6**$(PF_6)_4$ (300 MHz, DMSO, 298K)

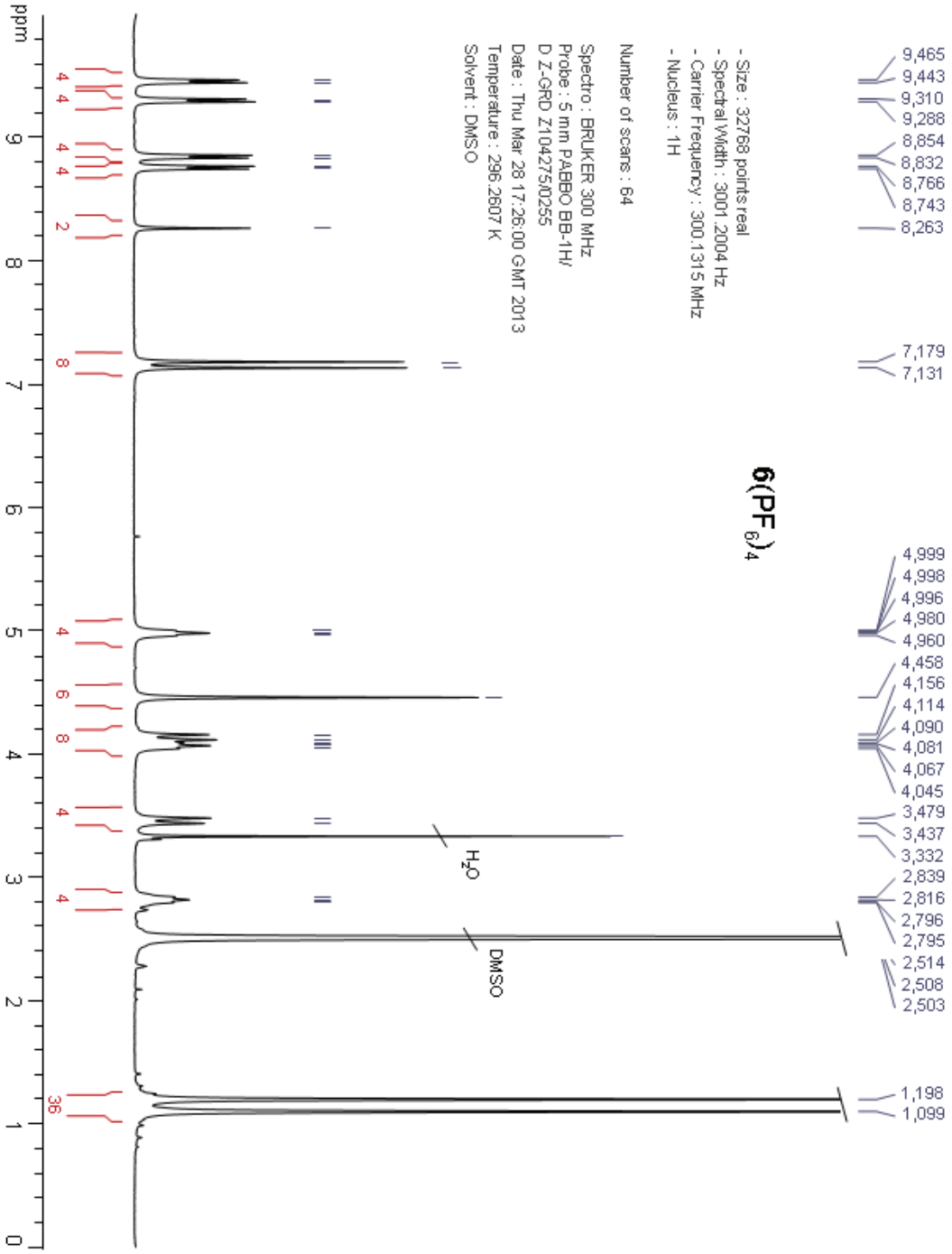

Fig. ESI 3 : ^{13}C NMR spectrum of **6**$(PF_6)_4$ (75 MHz, DMSO, 298K)

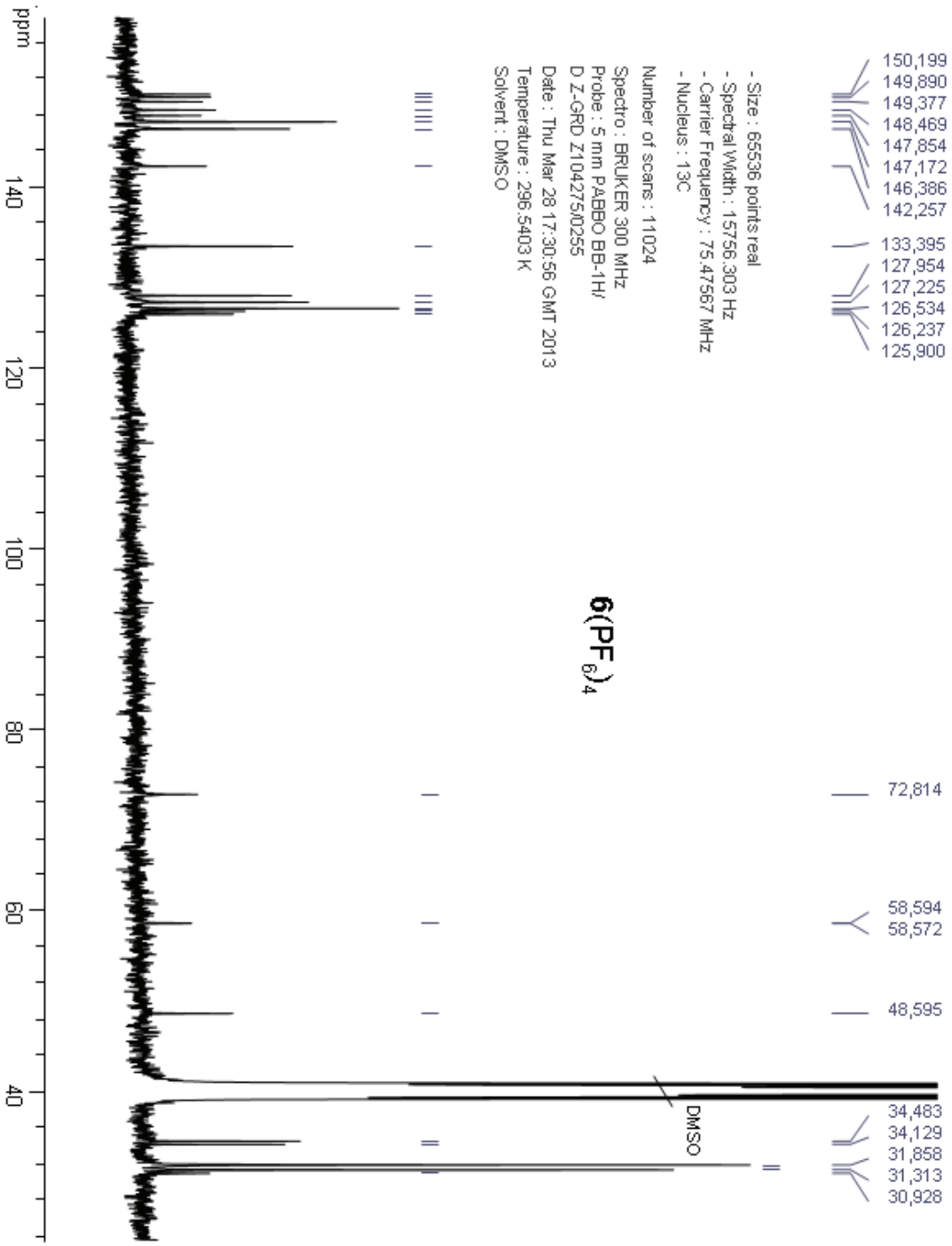

Fig. ESI 4 : ^{13}C NMR spectrum of **6**$(PF_6)_4$ (75 MHz, DMSO, 298K)

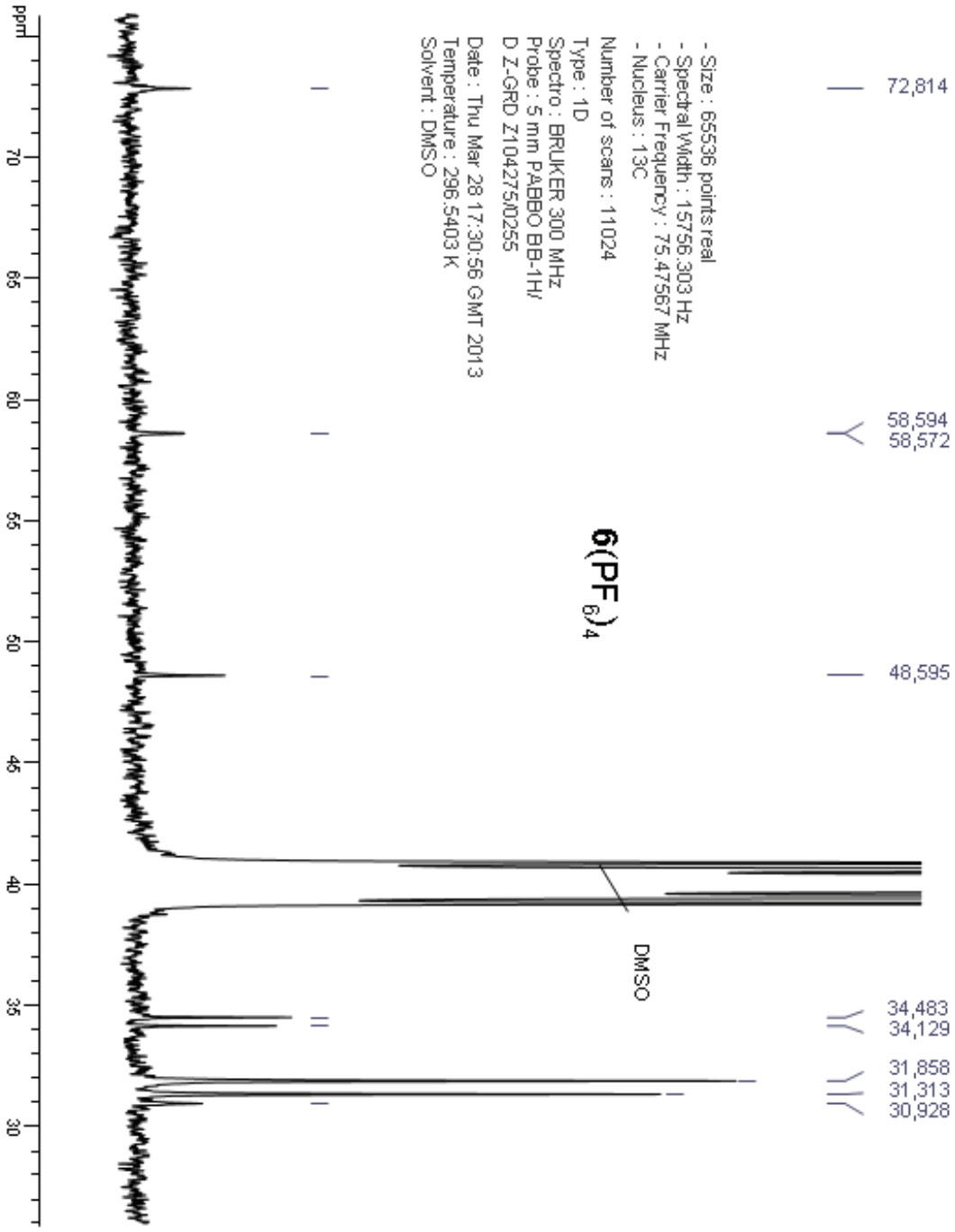

Fig. ESI 5 : ^{13}C NMR spectrum of **6**$(PF_6)_4$ (75 MHz, DMSO, 298K)

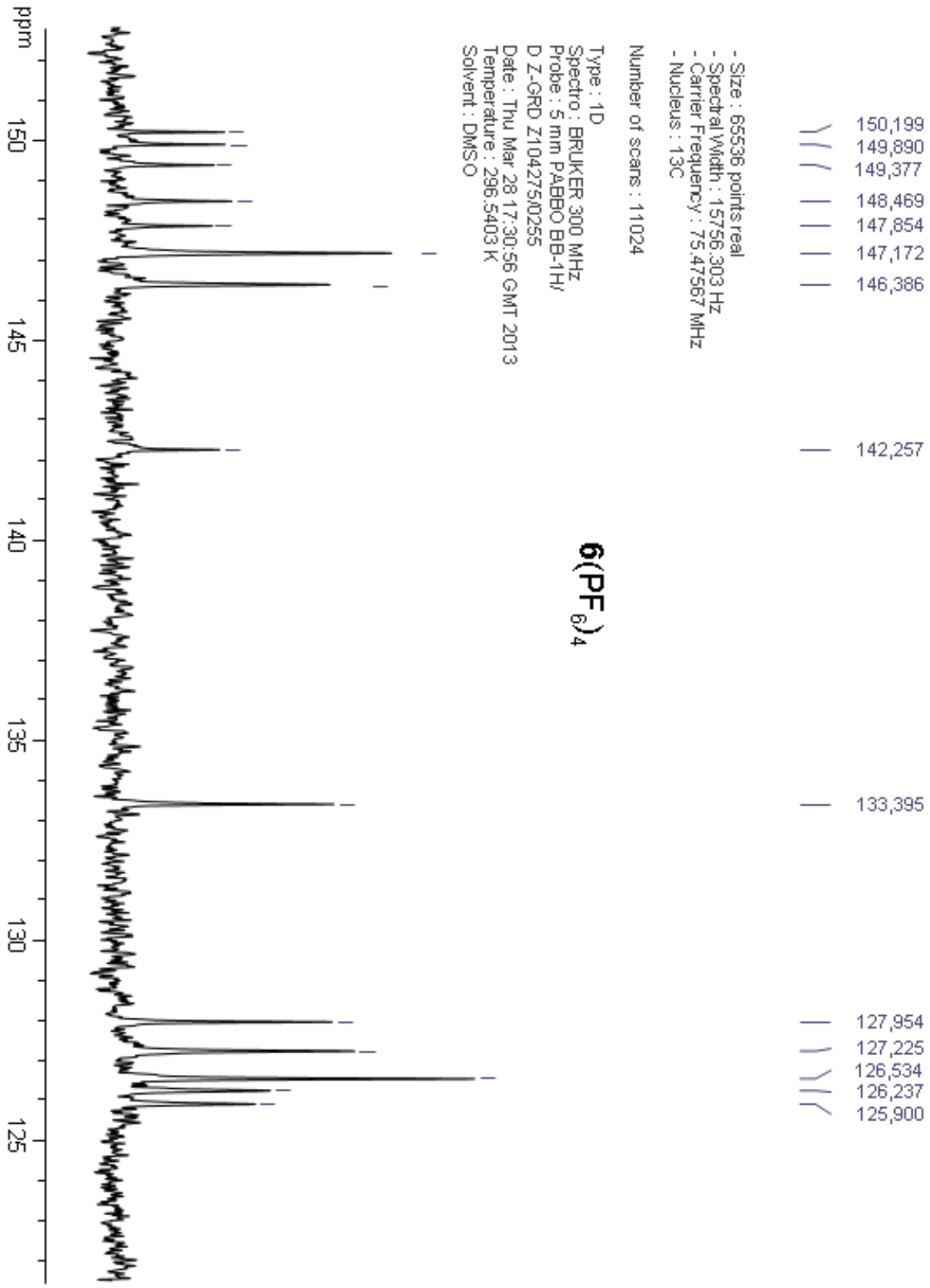

Fig. ESI 6 : LRMS spectrum of compound **5**$(PF_6)_4$

Calculated mass for **5**$(PF_6)_4$: $C_{70}H_{84}F_{24}N_4O_4P_4$; Exact Mass: 1624,51
Calculated mass for $[\mathbf{5}(PF_6)_3]^+$: $C_{70}H_{84}F_{18}N_4O_4P_3$; Exact Mass: 1479,54
Calculated mass for $[\mathbf{5}(PF_6)_3]^{2+}$: $C_{70}H_{84}F_{12}N_4O_4P_2$; Exact Mass: 1334,58
Calculated mass for $[\mathbf{5}(PF_6)_3]^{3+}$: $C_{70}H_{84}F_6N_4O_4P$; Exact Mass: 1189,61

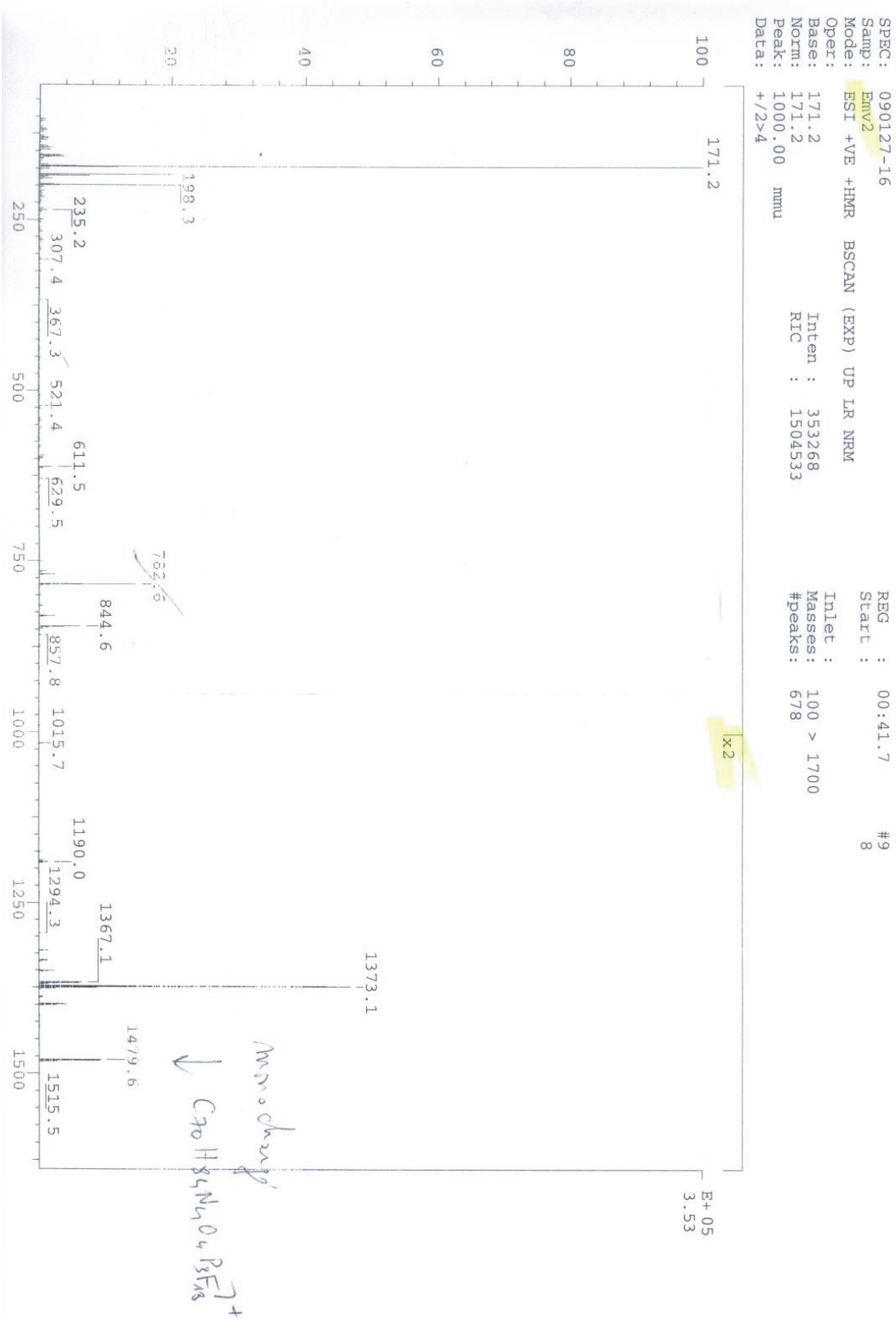

Fig. ESI 7 : HRMS spectrum of compound **6**$(PF_6)_4$

Calculated mass for $[\mathbf{5}(PF_6)_3]^+$: $C_{70}H_{84}F_{18}N_4O_4P_3$; Exact Mass: 1479,54

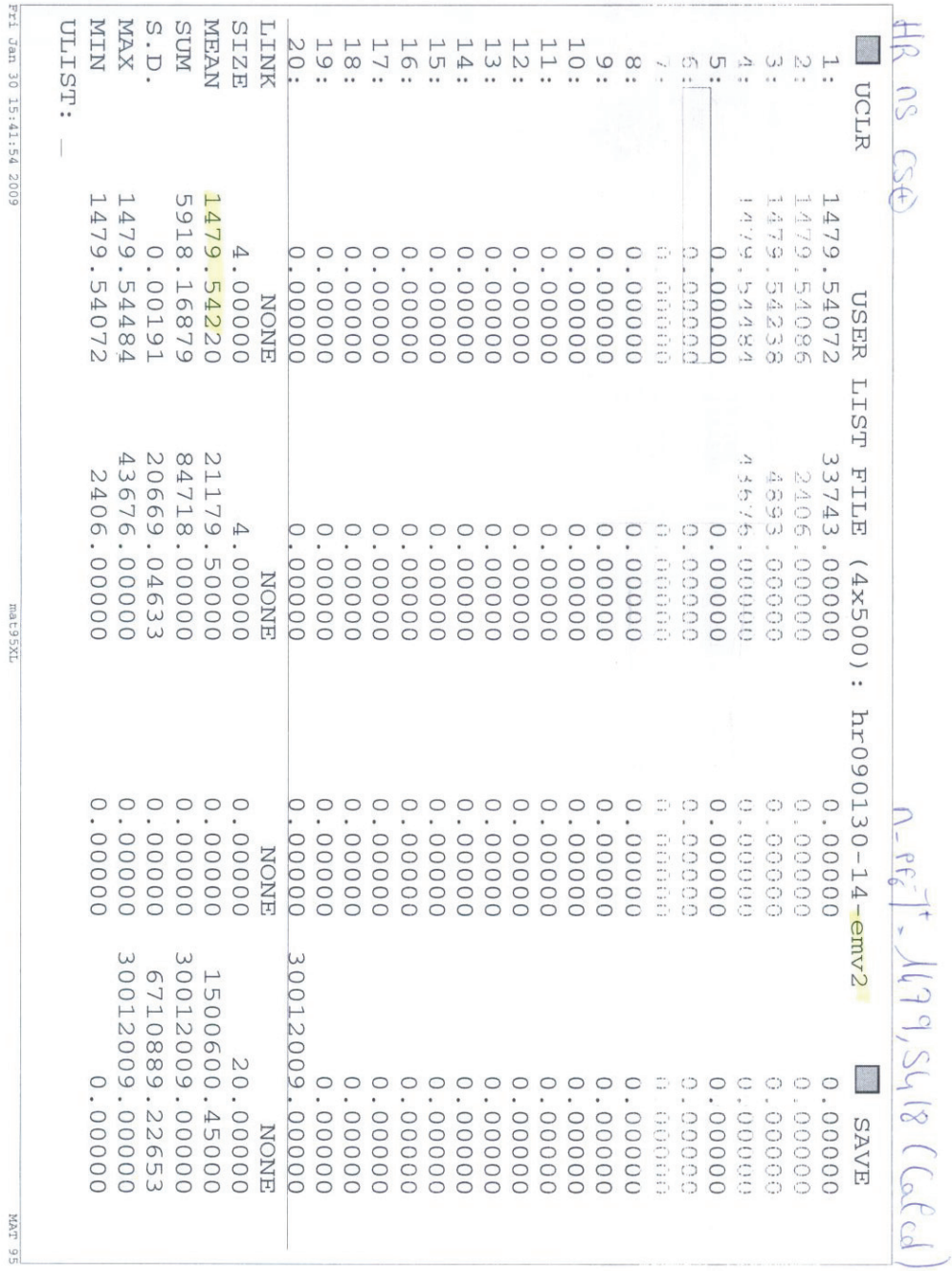

Fig. ESI 8 : ^{1}H NMR spectrum of **5**$(PF_6)_4$ (500 MHz, DMSO, 298K)

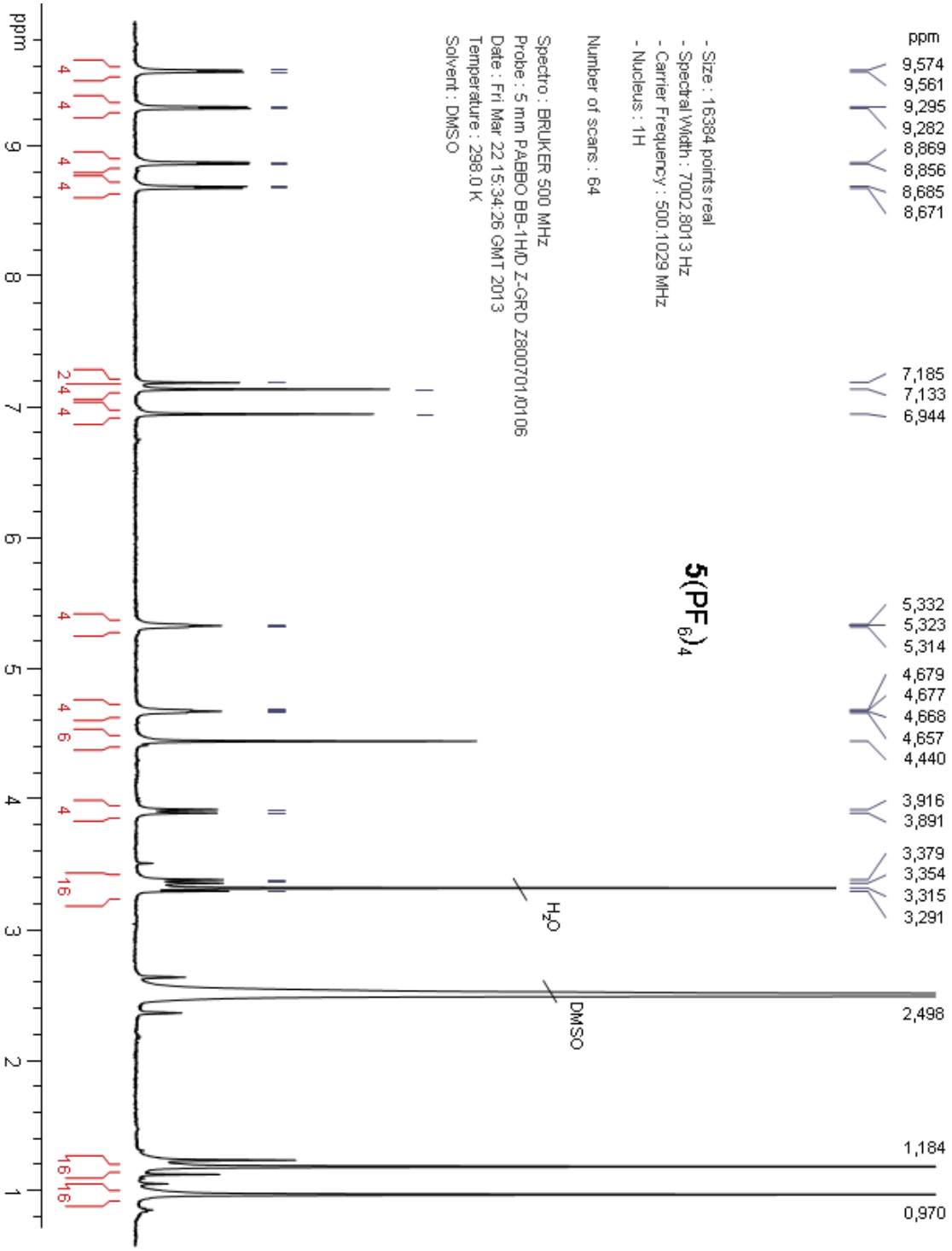

Fig. ESI 9 : ^{1}H NMR spectrum of **5**$(PF_6)_4$ (125 MHz, DMSO, 298K)

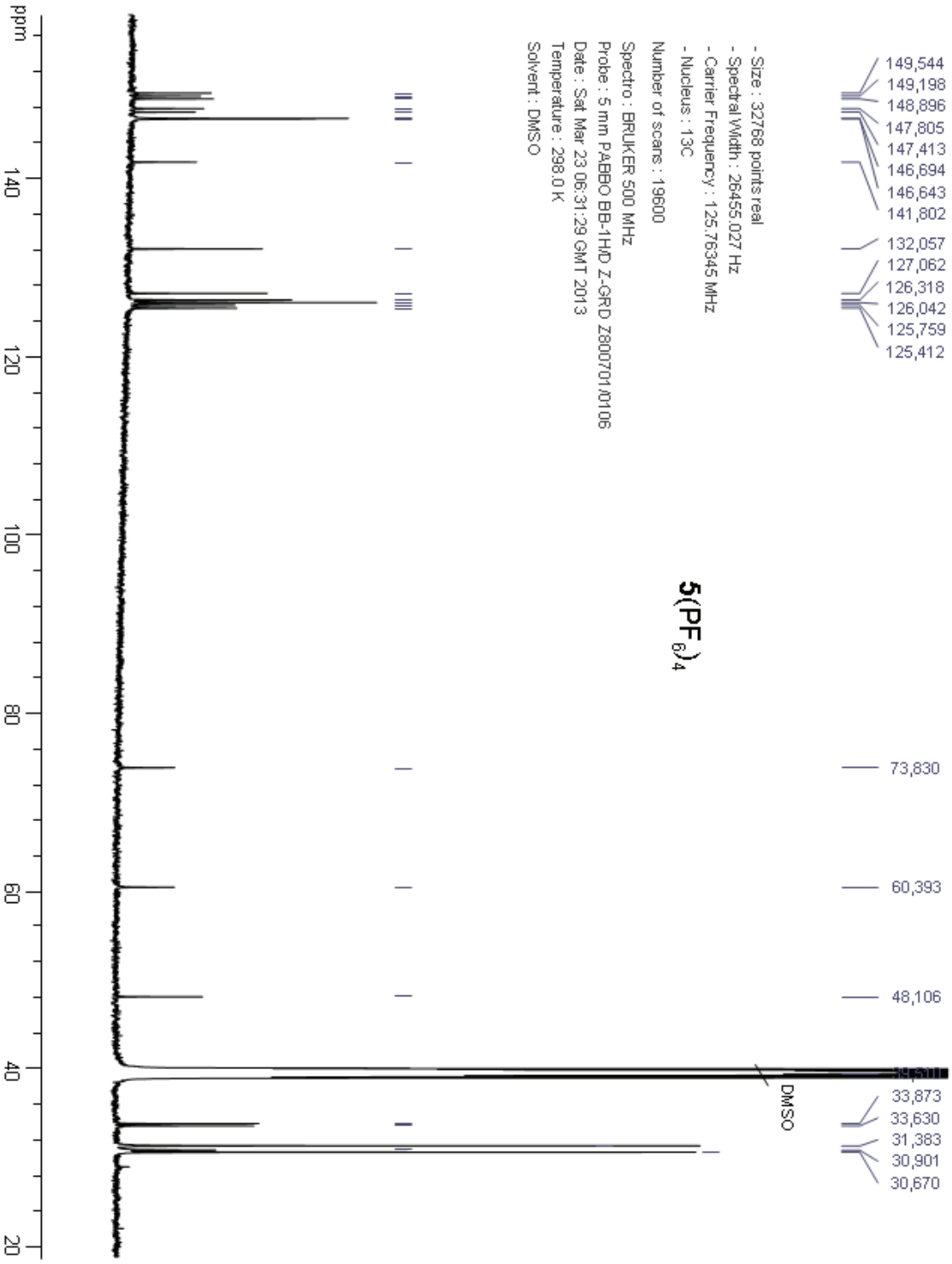

Fig. ESI 10 : ^{1}H NMR spectrum of **5**$(PF_6)_4$ (125 MHz, DMSO, 298K)

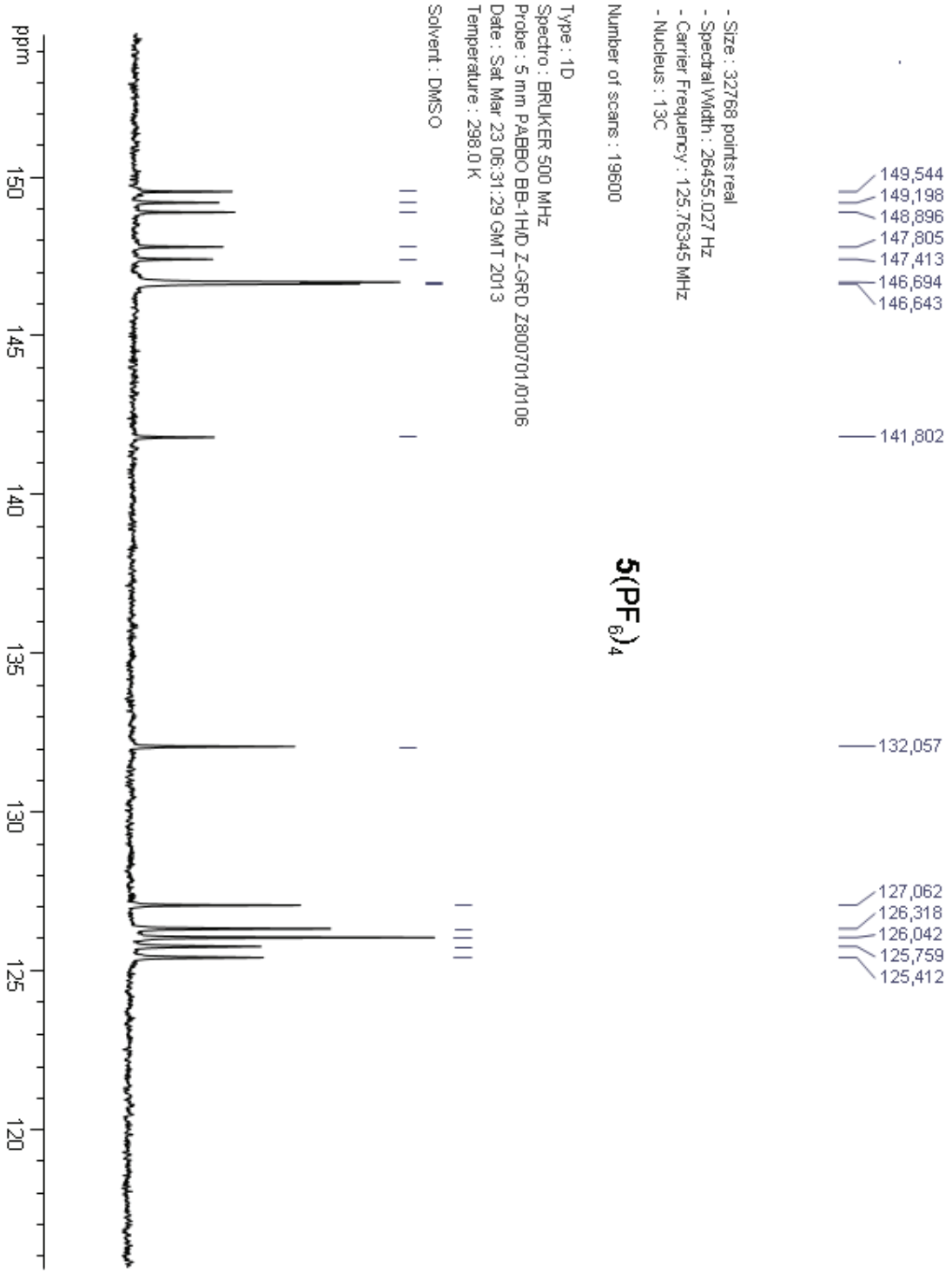

Fig. ESI 11 : ^{1}H NMR spectrum of **5**$(PF_6)_4$ (125 MHz, DMSO, 298K)

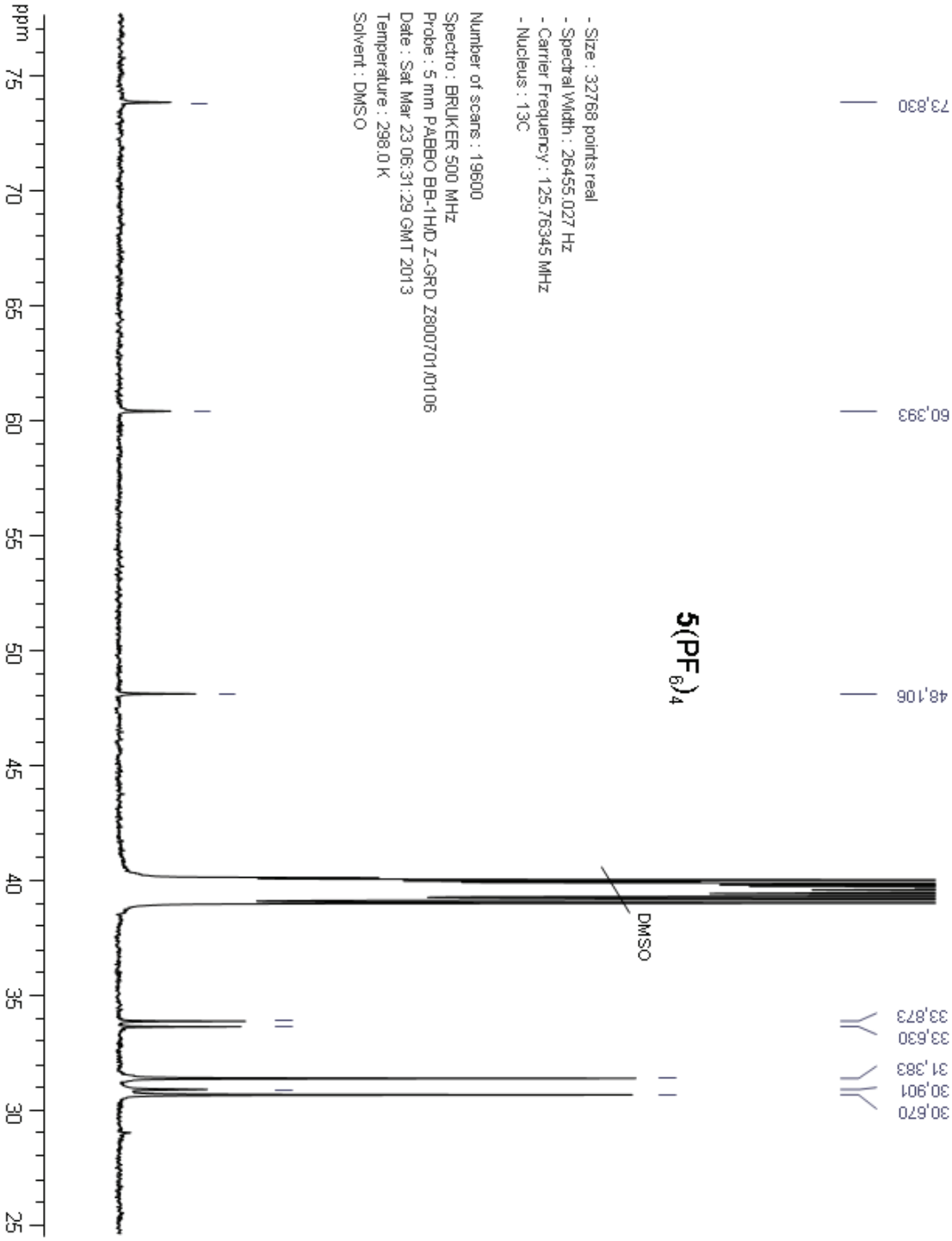

5$(PF_6)_4$ and **6**$(PF_6)_4$ were characterized using stationary and non stationary electrochemical methods. Cyclic voltammetry was used to calculate potential values (ΔE_P, E_{pa}, E_{pc}) and to examine the reversibility of each redox processes. Voltammetry recorded at rotating disks was used to confirm that both successive reduction waves involve the same number of electrons.

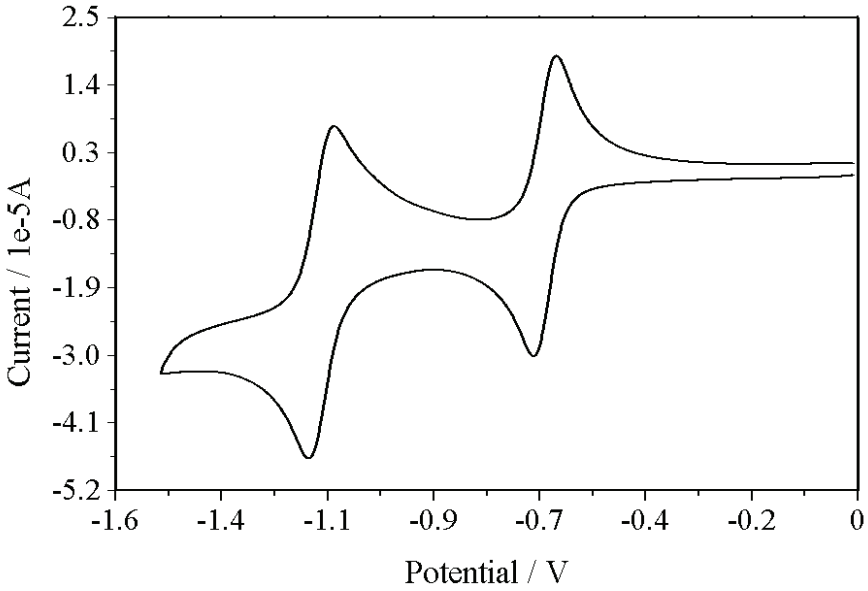

Fig. ESI 12 : Voltammetric curves of a 1 mM solution of **5**$(PF_6)_4$ in CH_3CN (TBAP 0.1 M) recorded by cyclic voltammetry at a stationary carbon working electrode (Ø = 3 mm, *E vs* Ag/Ag^+ (10^{-2} M), 298 K, ν = 0.1 $V \cdot s^{-1}$).

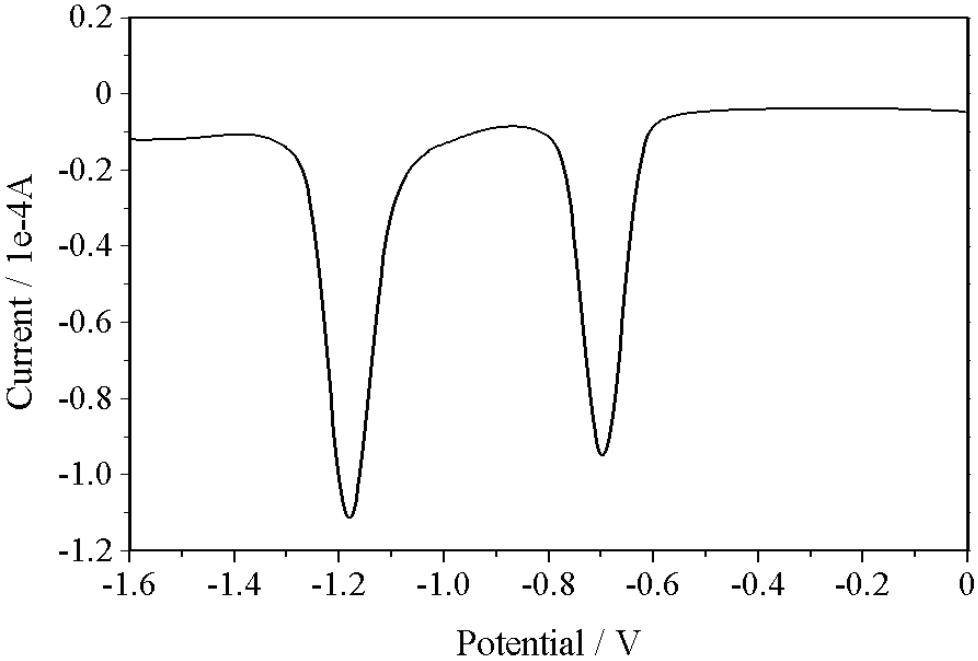

Fig. ESI 13 : Voltammetric curves of a 1 mM solution of **5**$(PF_6)_4$ in CH_3CN (TBAP 0.1 M) recorded by square wave voltammetry at a stationary carbon working electrode (Ø = 3 mm, *E vs* Ag/Ag^+ (10^{-2} M), 298 K, ΔE = 25 mV, IncrE = 4mV).

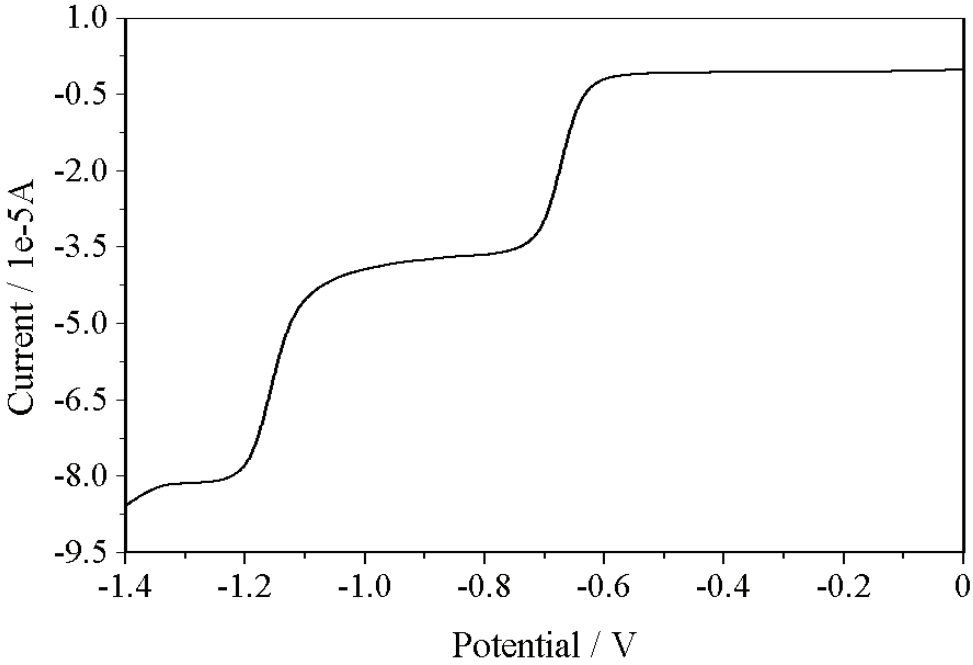

Fig. ESI 14 : Voltammetric curves of a 1 mM solution of **5**$(PF_6)_4$ in CH_3CN (TBAP 0.1 M) recorded by voltammetry at a rotating disk working electrode (Ø = 3 mm, *E vs* Ag/Ag^+ (10^{-2} M), 298 K, ν = 0.01 $V{\cdot}s^{-1}$).

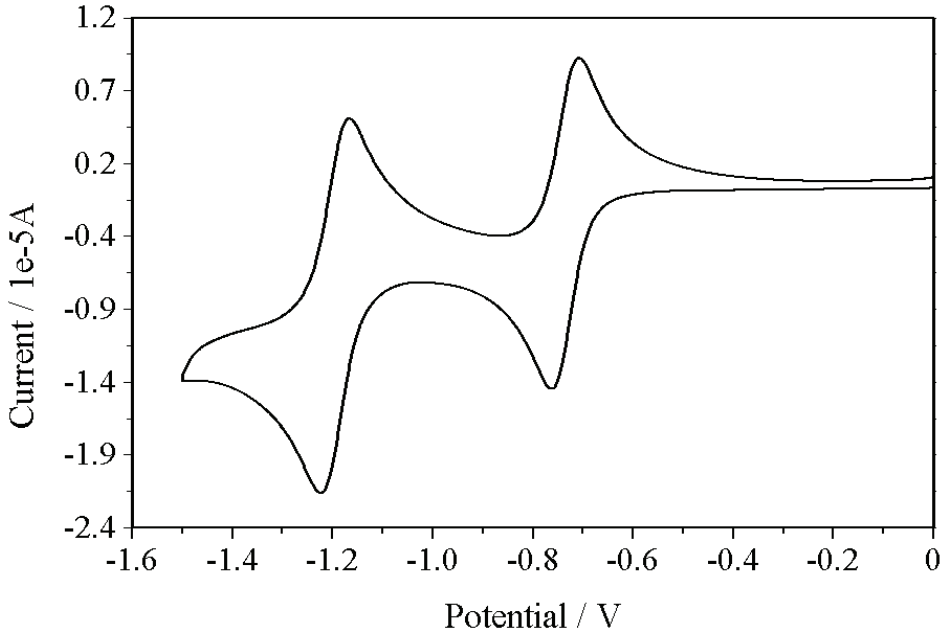

Fig. ESI 15 : Voltammetric curves of a 1 mM solution of **5**$(PF_6)_4$ in DMF (TBAP 0.1 M) recorded by cyclic voltammetry at a stationary carbon working electrode (Ø = 3 mm, *E vs* Ag/Ag^+ (10^{-2} M), 298 K, ν = 0.1 $V{\cdot}s^{-1}$).

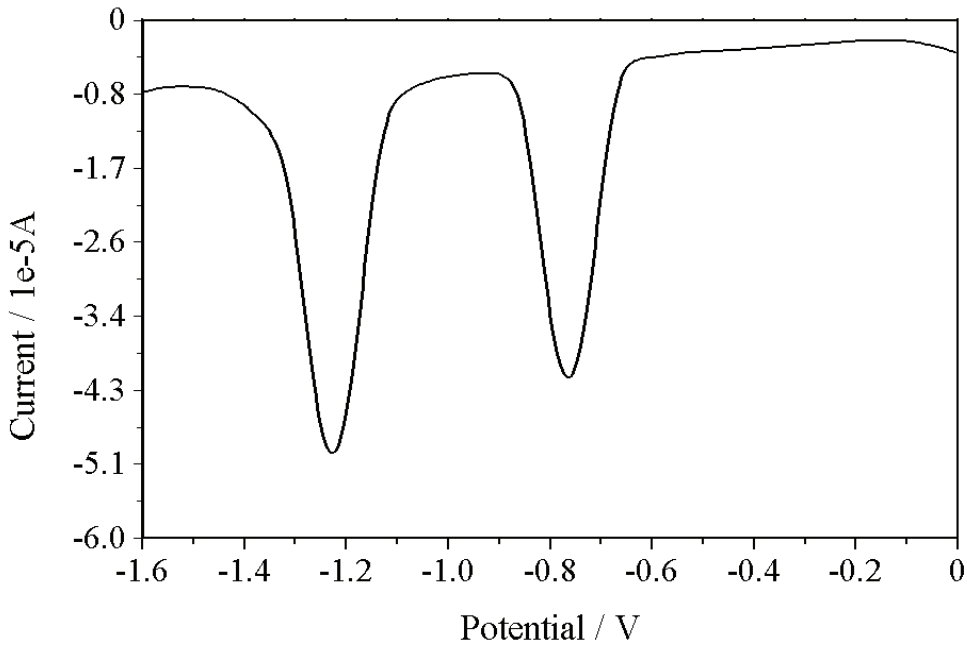

Fig. ESI 16 : Voltammetric curves of a 1 mM solution of **5**$(PF_6)_4$ in DMF (TBAP 0.1 M) recorded by square wave voltammetry at a stationary carbon working electrode (Ø = 3 mm, *E vs* Ag/Ag^+ (10^{-2} M), 298 K, ΔE = 25 mV, IncrE = 4mV).

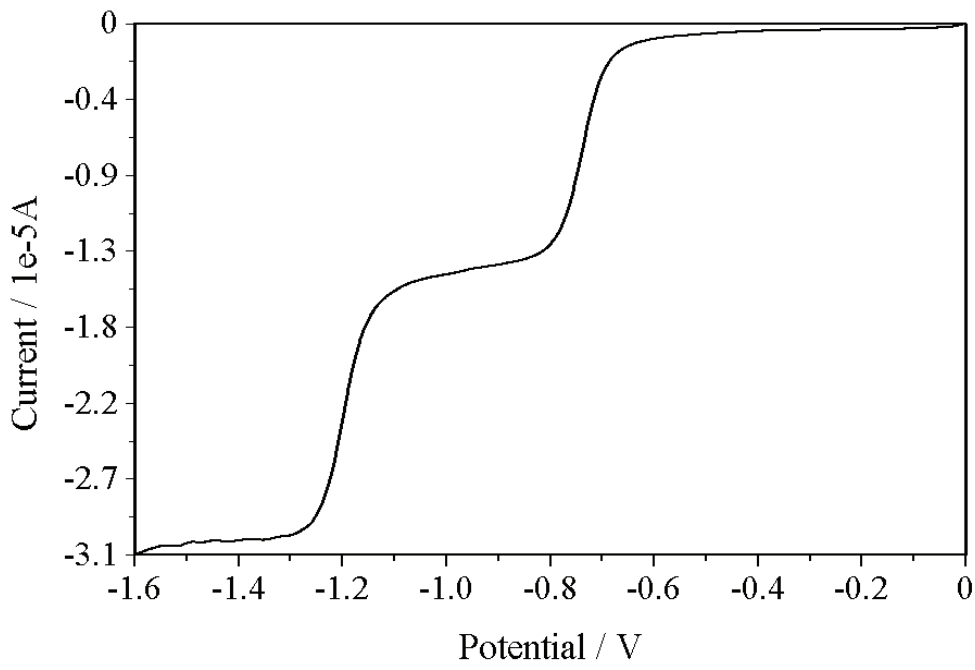

Fig. ESI 17 : Voltammetric curves of a 1 mM solution of **5**$(PF_6)_4$ in DMF (TBAP 0.1 M) recorded by voltammetry at a rotating disk working electrode (Ø = 3 mm, *E vs* Ag/Ag^+ (10^{-2} M), 298 K, ν = 0.01 $V \cdot s^{-1}$).

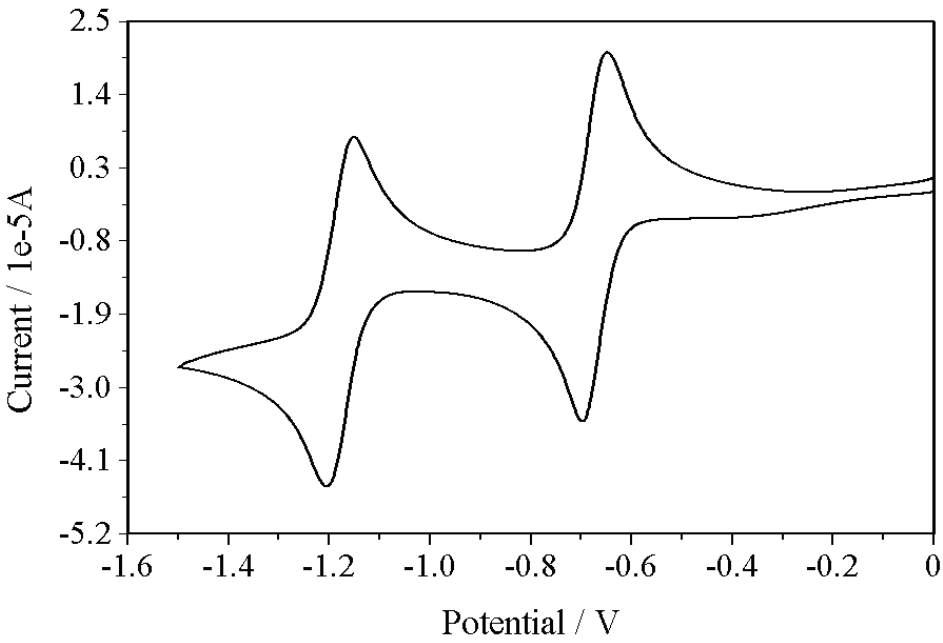

Fig. ESI 18 : Voltammetric curves of a 1 mM solution of **6**$(PF_6)_4$ in ACN (TBAP 0.1 M) recorded by cyclic voltammetry at a stationary carbon working electrode (Ø = 3 mm, *E vs* Ag/Ag^+ (10^{-2} M), 298 K, ν = 0.1 $V \cdot s^{-1}$).

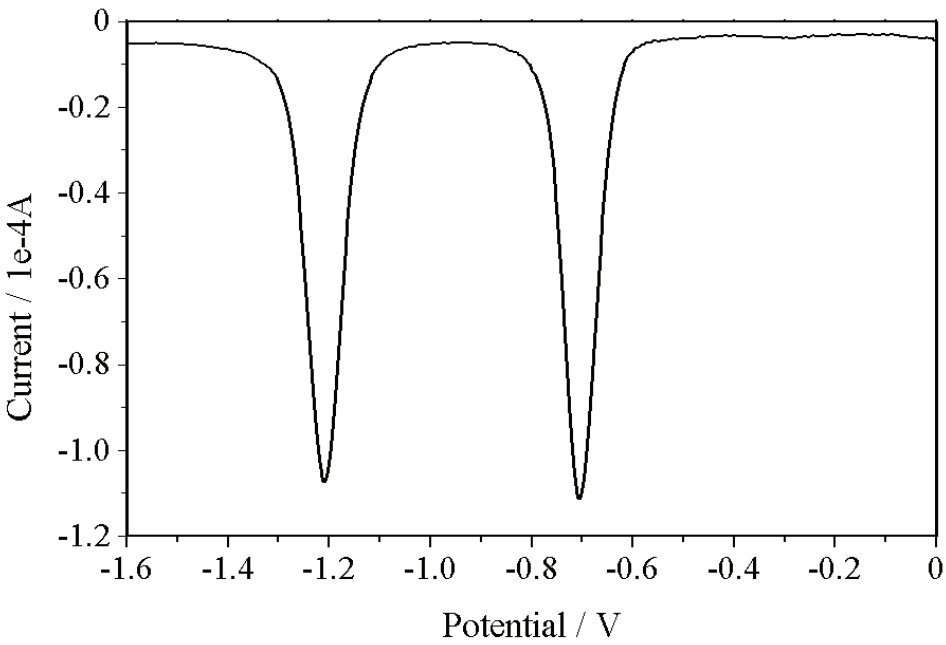

Fig. ESI 19 : Voltammetric curves of a 1 mM solution of **6**$(PF_6)_4$ in ACN (TBAP 0.1 M) recorded by square wave voltammetry at a stationary carbon working electrode (Ø = 3 mm, *E vs* Ag/Ag^+ (10^{-2} M), 298 K, ΔE = 25 mV, IncrE = 4mV).

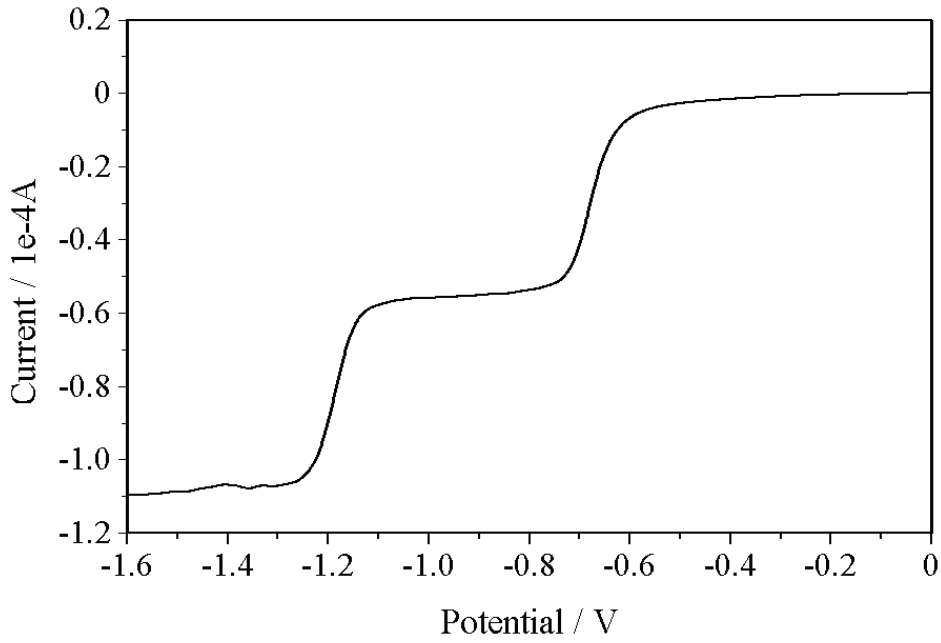

Fig. ESI 20 : Voltammetric curves of a 1 mM solution of **6**$(PF_6)_4$ in ACN (TBAP 0.1 M) recorded by voltammetry at a rotating disk working electrode (Ø = 3 mm, *E vs* Ag/Ag^+ (10^{-2} M), 298 K, ν = 0.01 $V{\cdot}s^{-1}$).

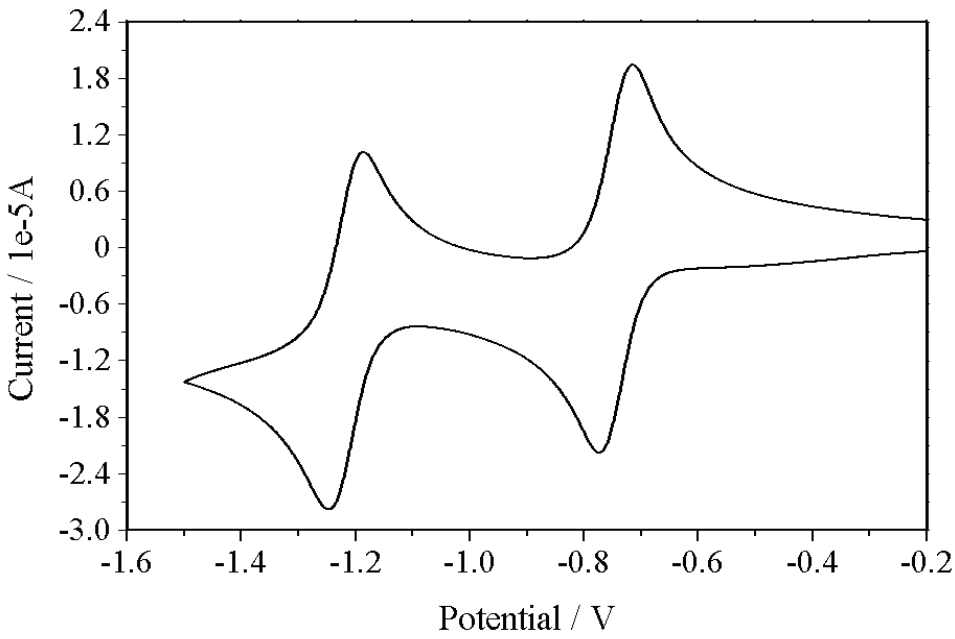

Fig. ESI 21 : Voltammetric curves of a 1 mM solution of **6**$(PF_6)_4$ in DMF (TBAP 0.1 M) recorded by cyclic voltammetry at a stationary carbon working electrode (Ø = 3 mm, *E vs* Ag/Ag^+ (10^{-2} M), 298 K, ν = 0.1 $V{\cdot}s^{-1}$).

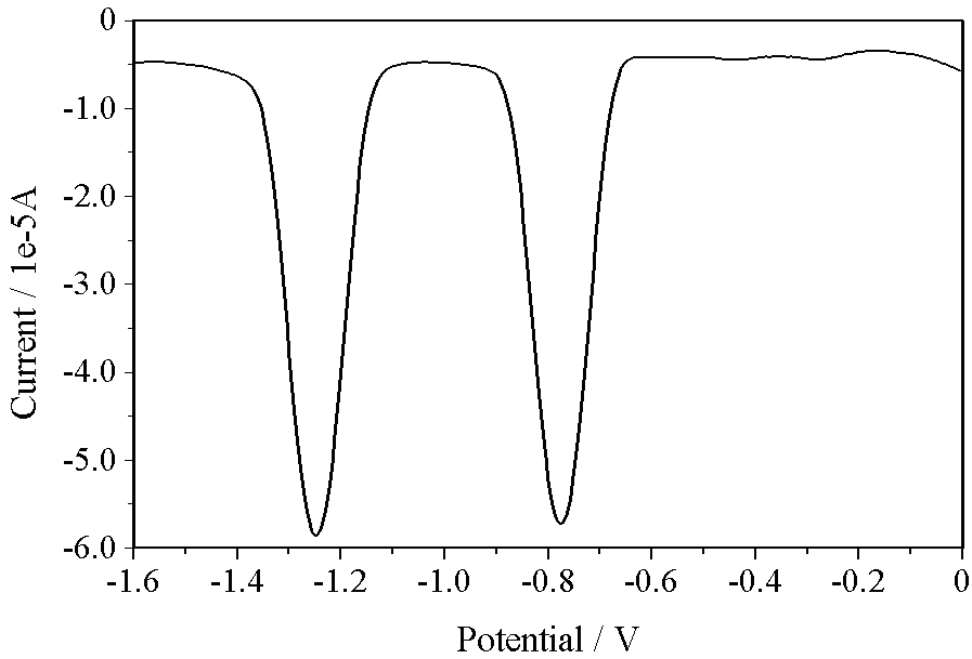

Fig. ESI 22 : Voltammetric curves of a 1 mM solution of **6**$(PF_6)_4$ in DMF (TBAP 0.1 M) recorded by square wave voltammetry at a stationary carbon working electrode (Ø = 3 mm, *E vs* Ag/Ag^+ (10^{-2} M), 298 K, ΔE = 25 mV, IncrE = 4mV).

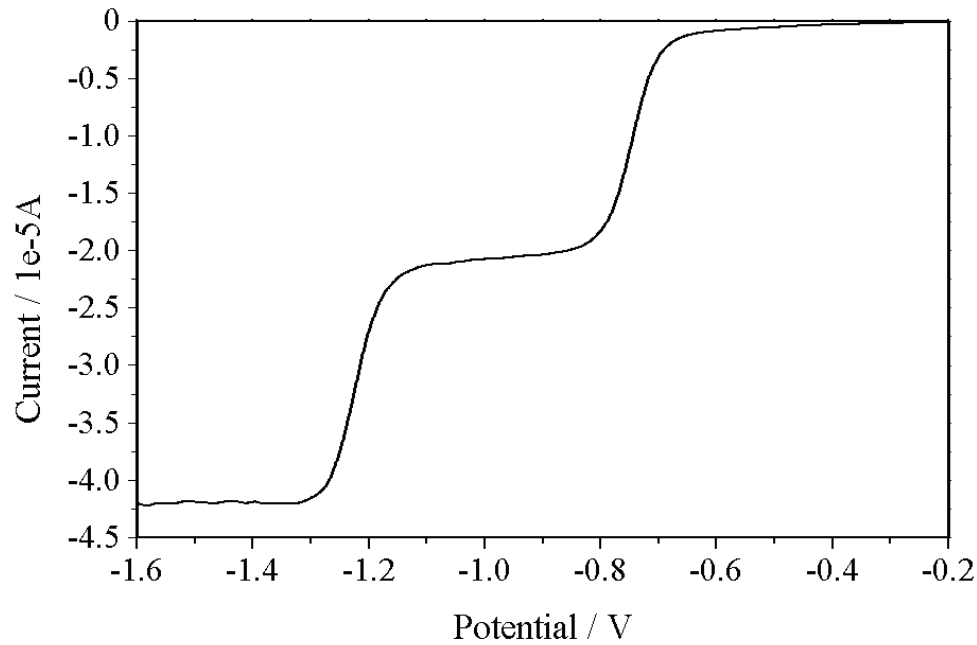

Fig. ESI 23 :Voltammetric curves of a 1 mM solution of **6**$(PF_6)_4$ in DMF (TBAP 0.1 M) recorded by voltammetry at a rotating disk working electrode (Ø = 3 mm, *E vs* Ag/Ag^+ (10^{-2} M), 298 K, ν = 0.01 $V \cdot s^{-1}$).

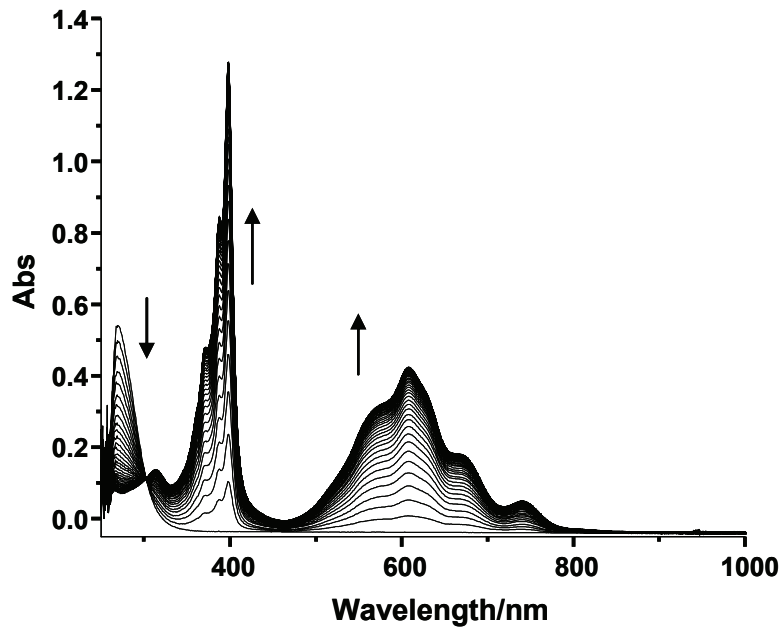

Fig. ESI 24 : UV-Vis spectra recorded during the exhaustive one-electron reduction of DMV(PF6)2 using a platinum plate working electrode whose potential was fixed at E_{ap} = –1 V (10^{-5} M in DMF/TBAP 0.1 M, l = 1 cm, E vs Ag/Ag^{+}).

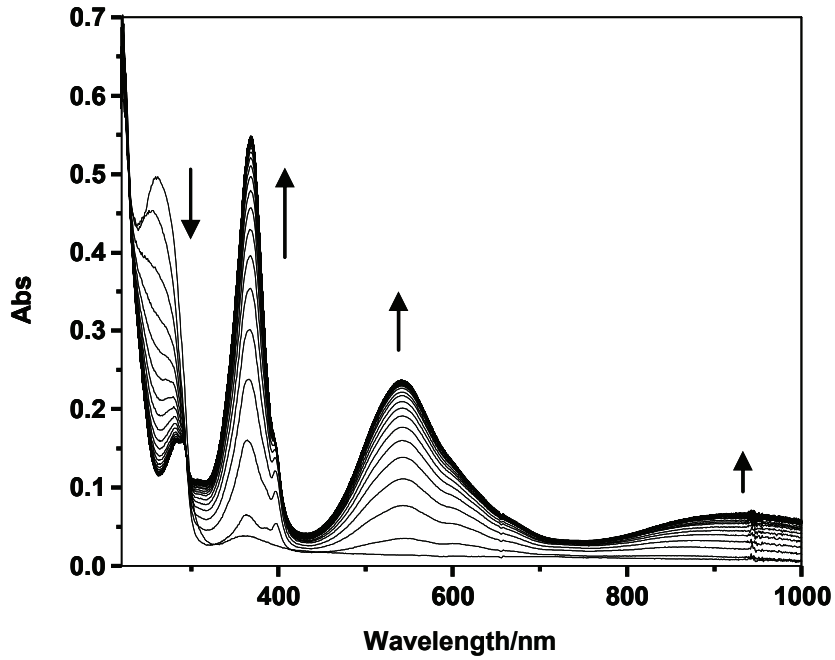

Fig. ESI 25 : UV-Vis spectra recorded during the exhaustive two-electron reduction **6**$(PF_6)_4$ using a platinum plate working electrode whose potential was fixed at E_{ap} = –1 V (10^{-5} M in ACN/TBAP 0.1 M, l = 1 cm, E vs Ag/Ag^{+}).

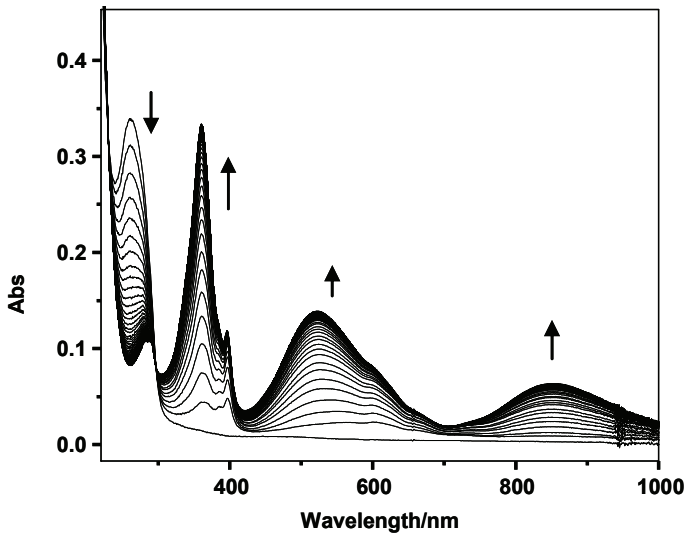

Fig. ESI 26 : UV-Vis spectra recorded during the exhaustive two-electron reduction **5**$(PF_6)_4$ using a platinum plate working electrode whose potential was fixed at $E_{ap} = -1$ V (10^{-5} M in ACN/TBAP 0.1 M, l = 1 cm, E vs Ag/Ag^+).

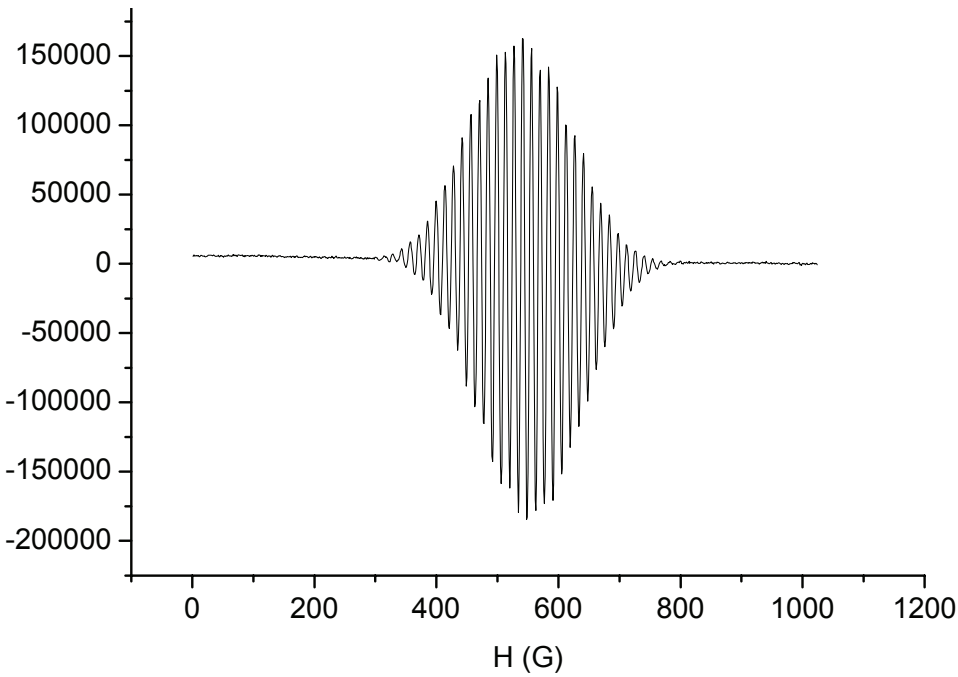

Fig. ESI 27 : X-band ESR spectra of **DMV**$^{+\bullet}$ recorded at room temperature, 10^{-4} M in viologen subunits dissolved in DMF + TBAP (0.1 M) (Microwave Power = 20 mW, Frequency = 9.42 Gz , Mod. Amp. =0.099mT, Mod. Freq 100 KHz)

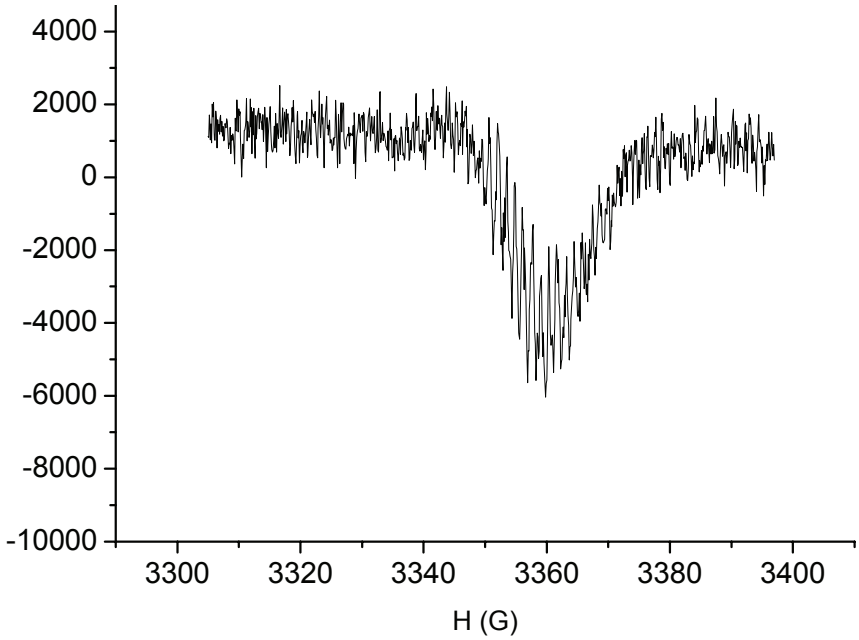

Fig. ESI 28 : X-band ESR spectra of $[\mathbf{6}^{2+}]_{dim}$ recorded at room temperature, 10^{-4} M in viologen subunits dissolved in DMF + TBAP (0.1 M) (Microwave Power = 20 mW, Frequency = 9.42 Gz , Mod. Amp. =0.099mT, Mod. Freq 100 KHz)

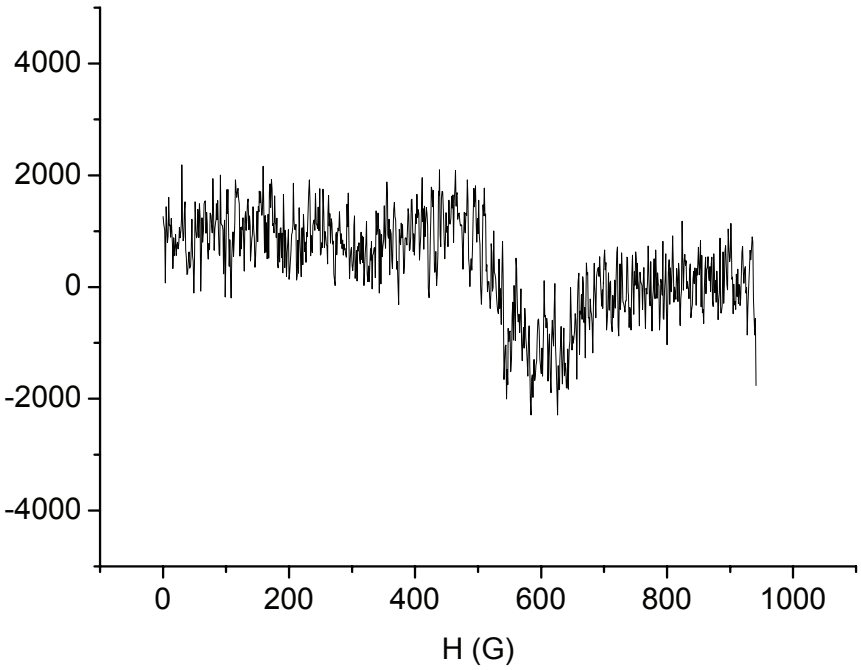

Fig. ESI 29 : X-band ESR spectra of $[\mathbf{5}^{2+}]_{dim}$ recorded at room temperature, 10^{-4} M in viologen subunits dissolved in DMF + TBAP (0.1 M) (Microwave Power = 20 mW, Frequency = 9.42 Gz , Mod. Amp. =0.099mT, Mod. Freq 100 KHz)

Fig. ESI 30 :Top and side views of the π-dimer complex found for **6**$^{4+}$ as a second, albeit less stable, minimum of the potential energy surface (ΔE ~20 kcal/mol) (Calculated at the BLYP-D3/DZVP level)